








Model of Milling the Root and Connecting Rod Necks of the Crankshaft for One Manufacturing Process

Vitaliy Kalchenko , Volodymyr Kalchenko , Nataliia Sira ,
Yaroslav Kuzhelnyi , and Vasyl Sklyar 

Chernihiv Polytechnic National University, 95, Shevchenko Street,
Chernihiv 14035, Ukraine

Abstract. During the crankshaft machining process, its axis of rotation does not coincide with the axis of rotation of the connecting rod neck. Therefore, the depth of a cut is always greater than the value of the allowable removed. It leads to uneven removal of allowance, reduces productivity and the quality of machining. The paper proposes a modular spatial model of removing the allowance and shaping of the root and connecting rod necks of the crankshafts during milling with crossed axes of the tool and part for one institution. Based on the developed model, the research of the formation of radical and connecting rod necks of a cranked shaft has been carried out. A method of milling the root and connecting rod necks of the crankshaft with crossed tool axes and parts has been presented, where the angle of rotation of the tool is selected from the condition of ensuring the straightness of the forming neck. In this case, the rough allowance is removed at the end, and the final allowance and calibration - the periphery of the cutter plate, which rotates and simultaneously performs the vertical and transverse movement, and the shaft performs a uniform rotation. The proposed method of milling provides stabilization of the depth of a cut along with the profile of the connecting rod necks, the area of the removed allowance, and the feed rate along the contour of the part.

Keywords: Milling · Crankshaft milling · Crossed axes · Root necks · Modular modeling

1 Introduction

Automotive, tractor, shipbuilding, and other machine-building industries are characterized by extensive use of parts with complex profile surfaces. Such surfaces include, for example, crankshaft necks, camshaft cams, and the like. It is necessary to ensure high productivity of their machining with high manufacturing accuracy in manufacturing such parts.

The necks of the crankshaft are processed at the machine-tool plant “Shlif-verst” on machines of models 3411, 3D4230, 3D4231, 3DB23, LT-235. All root necks of a shaft are ground for one establishment. During the machining of each connecting rod neck to align its axis of rotation with the axis of rotation of the machine spindle, the crankshaft

is reinstalled, which causes an imbalance. It reduces the productivity and accuracy of machining.

For the first time, root and connecting rod necks were machined by Junker (Germany) on a circular grinder in one place. The contact of the neck with the circle is due to the reciprocating motion of the tool, which provides a running-in of the neck for one revolution of the shaft.

One of the productive ways to process complex profile parts is milling. In [1], the influence of high-speed milling on pre-matured tool life is investigated. Paper [2] performs an overview of cutting characteristics of high speed and CNC milling with potentials and applicability for high-performance material. In [3] presents a review of the research work published over the past decade considering five main domains in the free-form surface milling process, which enhance accuracy, machinability, productivity, and machining economy. From the perspective of complex parts robotic milling, this paper [4] focuses on machining process planning and control techniques. Therefore, the development and study of spatial modular models of the removal of allowance and shaping the necks of the crankshafts in milling with crossed axes of the tool and part for one institution is an urgent task. The solution of this task will increase the accuracy of the root and support necks of the crankshafts and the productivity of their machining.

2 Literature Review

Studies of the accuracy of crankshaft machining processes are given in [1, 5–7]. Thus, in [5], an approach to determining the cutting force during machining of crankshafts has been presented, which allows determining the influence of technological parameters on the power characteristics of the cutting process accurately. In [6], researched how to avoid chatter in crankshaft Tangential Point Tracing grinding, Stability lobe diagram has been developed based on the dynamic model to predict chatter. In [7], to improve the crankshaft's accuracy of the crankshaft an automatic alignment approach and apparatus have been proposed and integrated into the non-circular grinder. In [8], the design of a lunette for CNC grinding machines, on which the machining of the crankshaft root and connecting rod necks is carried out, has been proposed. The construction design of the device allows for compensating the influence of the cutting force on the elastic strain of the part, depending on the change in its rigidity. In [9], for the mass production of vehicle-engine crankshafts, a new in-situ roundness measurement strategy has been proposed with high scanning speed. In [10], the process of milling the connecting rod necks of the crankshaft based on the machine's power consumption has been optimized. In [11], a series of experiments were performed to investigate the machinability in crankshaft pin journal path-controlled grinding of 40Cr using vitrified bonded cubic boron nitride (CBN) abrasive. However, the works do not consider methods of single-pass machining of crankshafts.

In [12], the models of milling the support necks and camshaft cams for one institution have been developed. The disadvantage of this method when machining the necks of the crankshaft is the uneven rotation of the part, which will cause the formation error.

In works [13–15] to increase the efficiency of machining and manufacturing crankshafts, their optimization has been carried out. In [13], computer-aided modeling using CATIA and optimization analysis of crankshaft is used to evaluate and compare the fatigue performance of different materials of automotive crankshafts. For the crankshaft system of a four-cylinder in-line gasoline engine, a procedure to build the finite element model is presented [14]. Paper [15] presents the stochastic process for reliability assessment based on the fatigue life data under random loading for structural health monitoring of an automobile crankshaft due to fatigue failure. However, the presented models do not consider the processes of removal of the allowance and the movement of the formation of the crankshafts.

There are no spatial modular models of the processes of removal of allowance and shaping in one-pass milling of the root and connecting rod necks of crankshafts with crossed tool axes and parts in the known works.

3 Research Methodology

The scheme of the process of milling the crankshaft 1 for one institution with crossed axes of it and the cutter 2 is presented in Fig. 1.

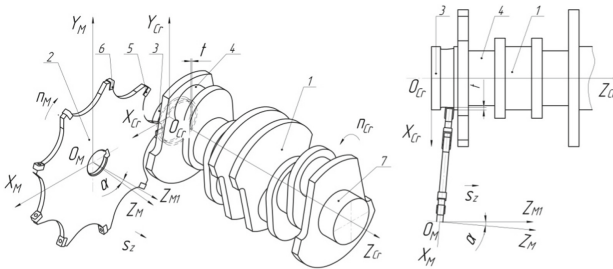


Fig. 1. Crankshaft milling scheme with crossed tool axes and parts.

When machining the root 3 and connecting rod 4 necks of the shaft 1 (Fig. 1), cutter 2 is rotated around the $O_M Y_M$ axis at an angle α , which is selected from the condition of ensuring the required accuracy of the end surfaces of the neck flanges:

$$\alpha = \operatorname{arctg} \frac{2\delta}{-2r_p}, \tag{1}$$

where δ – is the permissible deviation from the perpendicularity of the end surface of the crankshaft neck; H – the difference between the diameters, which determines the height of the flange; r_p – is the radius of curvature of the radius edge of the cutter blade.

Milling of the crankshaft 1 is carried out by a cutter 2, which in the middle of the root neck 3 cuts into the entire depth of cut t (Fig. 1) and moves along the axis $O_{Cr}Z_{Cr}$ coordinate system of the part with the supply s_z . Cutting of a mill in the middle of a

neck is carried out to uniform wear of plates of the tool. The rough allowance is removed by the end face of plate 5 (Fig. 1), and the periphery of the plate performs finishing and calibration.

When machining the neck, due to the crossing of the axes $O_M Z_{M1}$ cutter 2 and $O_{Cr} Z_{Cr}$ crankshaft 1 (Fig. 1), there is a deviation from the straightness of the forming neck. The point of intersection D (Fig. 2) of the axes of cutter 2 and part 1 is at a distance $(B-h)$. To ensure the straightness of the forming neck, the axis of rotation of the cutter is shifted in the direction of the axis $O_{Cr} Z_{Cr}$ due to the vertical movement of the tool in the direction opposite to the axis $O_{Cr} X_{Cr}$. In position II (Fig. 2), the distance from the point $D1$ of crossing the axes to the end of the tool decreases and is $(B-h1)$. Consequently, the error of shaping is reduced. Therefore, to ensure the straightness of the generating necks of the crankshaft, the point of intersection of the D axes (Fig. 2) is moved to the extreme position to the end of the tool in the direction of the axis $O_{Cr} Z_{Cr}$.

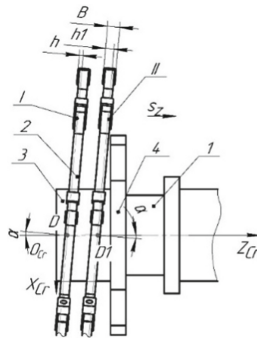


Fig. 2. The scheme of displacement of the cutter to ensure the straightness of the generating neck of the crankshaft.

When machining the root neck 3 of the crankshaft (Fig. 3), cutter 2 is given rotation n_M . To ensure the straightness of the neck profile, the point of intersection of the axes during machining is shifted to the extreme position in the direction of the end face of the flange of the part (Fig. 2).

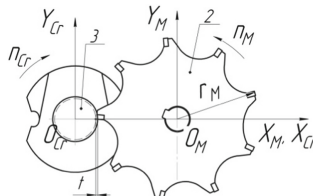


Fig. 3. The scheme of milling of radical necks of a cranked shaft.

When machining the end surface of the neck, the shaft must make at least one turn. After machining the root neck 3, the cutter is moved in the vertical direction of the $O_{Cr}Y_{Cr}$ axis to the height of the location of the connecting rod neck 4 (Fig. 1). In the middle of the connecting rod neck, the cutter cuts into the value of the allowance t , and the process of its machining begins (Fig. 4).

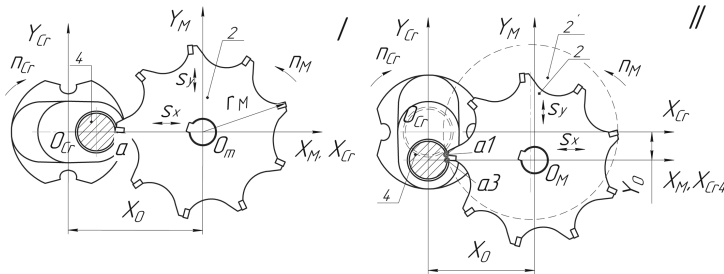


Fig. 4. The scheme of milling of connecting rod necks of a cranked shaft.

Since the axis of rotation of the connecting rod neck 4 and the axis of rotation of the crankshaft 1 (Fig. 1) are in different planes, with uniform rotation of the crankshaft, the point of contact a (Fig. 4, I) of the cutter plate 2 with the part moves relative to the horizontal plane of the connecting rod neck. And due to the transverse movement s_x of the cutter (position 2') occupies the position $a1$ (Fig. 4, II). It ensures the running-in of the neck profile 4.

Synchronous vertical movement s_y of the cutter 2 (Fig. 4, II) ensures the constancy of the location of the contact point $a3$ in the plane passing through the axis of rotation of the connecting rod neck and the cutter. Due to this, the cutting depth t (equal to the value of the allowance), the feed rate along the contour, and the area of the removed allowance remain unchanged during machining.

After machining the connecting rod neck 4 of the crankshaft (Fig. 1), the halves of other root and connecting rod necks are milled according to the described method. After finishing the machining of the half of the root neck 7, the cutter is rotated to the opposite angle $-\alpha$ and the other halves of the root and connecting rod necks of the crankshaft are machined in the feed direction opposite to s_z .

Uniform circular crankshaft feed with simultaneous vertical and transverse tool movements when milling connecting rod necks ensures constant cutting depth and feed rate along the contour. It increases the accuracy of machining of the connecting rod necks of the crankshafts and the possibility of increasing the productivity of their machining by increasing the frequency of rotation of the part.

Set the tool surface with the radius vector \vec{r}_M of the cutter as the product of the matrices M2, M3 (movement along the $O_M Y_M$ and $O_M Z_M$ axes, respectively), and M6 (on the rotation around the $O_M Z_M$ axis (Fig. 1)):

$$\overline{r}_M = M3(Z_M) \cdot M6(\beta) \cdot M2(r_M) \cdot \overline{e}4, \quad (2)$$

where $Z_M = 0 \dots B$ – the linear coordinate of the cutting plate of the cutter, varies from 0 to the width B of the plate; r_M – radius of a mill; $\beta = 0 \dots 360^\circ$ – angular coordinate, which sets the profile of the cutter; $\overline{e}4$ – radius-vector of the beginning of the coordinate system of the cutter.

The nominal surface \overline{r}_{Cr} of the crankshaft is given by the product of the radius vector \overline{r} of the cutter and single-coordinate displacement matrices M1 (movement along the $O_M X_M$ axis), M2, M3, and turns M5 (rotation around the $O_M Y_M$ axis), M6:

$$\overline{r}_{Cr} = M3(Z_{Cr}) \cdot M6(\delta_{Cr}) \cdot M1(X_0) \cdot M5(x) \cdot M2(Y_0) \cdot \overline{r}_M, \quad (3)$$

where X_0, Y_0 – is the wheelbase of the cutter and the part in the horizontal and vertical planes, respectively; δ_{Cr} – angular coordinate, which sets the profile of the shaft; Z_{Cr} – coordinate, which describes the movement of the cutter along the axis $O_{Cr} Z_{Cr}$ relative to the part (feed).

Since the machined surface depends on six parameters (2), we connect the feed Z_{Cr} , wheelbase $X_0(\delta_{Cr}), Y_0(\delta_{Cr})$ cutters, and parts in the horizontal and vertical planes using Eqs. (3)–(6):

$$Z_{Cr} = \delta_{Cr} \cdot \frac{Sz}{2 \cdot \pi}, \quad (4)$$

$$Y_0(\delta_{Cr}) = r_{ec} \cdot \sin \delta_{Cr}, \quad (5)$$

$$X_0(\delta_{Cr}) = r_M + r_{Cr2} + r_{ec} \cdot \cos \delta_{Cr}, \quad (6)$$

$$\overline{V} \cdot \overline{n} = 0, \quad (7)$$

where r_{ec} – eccentricity (distance between the axes of rotation of the connecting rod and the root neck of the crankshaft); r_{Cr2} – the radius of the connecting rod neck of the crankshaft; \overline{n} – is the unit vector of the normal to the tool surface; \overline{V} – is the vector of the speed of relative movement of the tool in the coordinate system of the crankshaft.

The crossing of the axes of the cutter and the crankshaft causes a deviation from the perpendicularity of the end surface of the workpiece. To determine the end profile, find the line of intersection of the part with the coordinate plane $Z_{Cr} O_{Cr} Y_{Cr}$ using the equations:

$$B_{Cr}(x, \delta_{Cr}) =: \text{root}(\text{Det}(\delta_{Cr}, x)_3, \delta_{Cr}), \quad (8)$$

$$\text{Pr}_{Cr}(x) =: \text{Det}(\delta_{Cr}(i, 5 \cdot ^\circ), i). \quad (9)$$

Specific productivity of milling Q , which determines the volume of metal cut by the tooth within the point x :

$$Q(x) = \int_{\beta_1(x)}^{\beta_2(x)} (Vn(\beta, x) - y_v) \cdot r_M(x) \cdot d\beta, \tag{10}$$

where $\beta_1(x), \beta_2(x)$ – the angles of entry and exit of the cutter's tooth from the workpiece on its radius $r_M(x)$; y_v – system flexibility.

4 Results

Calculations and construction of models have been performed using the mathematical package Mathcad.

Using Eqs. (1)–(6), the contact line of the cutter and the neck of the crankshaft have been obtained (Fig. 5). It starts from some point x_{rk} at the end of the plate 5 of the cutter 2 (Fig. 1), passes through the radius of its rounding (coordinate from x_{rk} to x_{r0}), and ends at the periphery at the point of intersection of the axes of the cutter and the neck of the crankshaft.

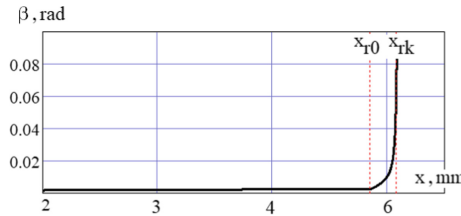


Fig. 5. Contact line of the cutter tooth and parts along with the tool profile.

The contact spot 3 (Fig. 6) of the cutting edge of cutter 2 and the neck of the crankshaft 1 is formed by the intersection of lines 4, 5, 6. Where 4 – is the contact line of the cutting edge of the cutter and the shaft neck (Fig. 5), 5 – is the line of intersection of the tooth cutter and end face of the machined surface, 6 – line of intersection of the outer cylindrical surface of the neck of the shaft and the cutter.

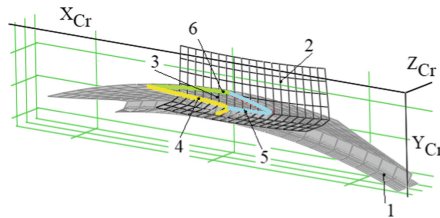


Fig. 6. Contact spot of the cutter tooth and the crankshaft neck.

Using Eqs. (7)–(8), the profile of the treated end surface of the crankshaft collar (Fig. 7) has been obtained.

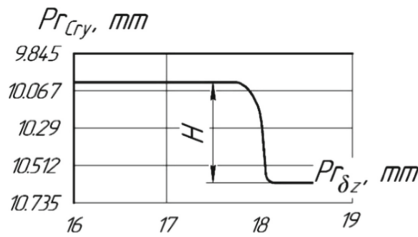


Fig. 7. The profile of the end face of the crankshaft neck.

Synchronous vertical and transverse movement of the cutter, described by Eqs. (5), (6) of the movement of the center of the cutter, ensure the constancy of the point of contact a3 (Fig. 4) in the plane passing through the axis of rotation of the connecting rod neck and cutter. Due to this, the depth of cut t (equal to the allowance value) (Fig. 8, a), the area of the removed allowance, and the feed rate along the contour of the part remain unchanged during the machining process. And, consequently, the accuracy of shaping the connecting rod necks of the crankshaft increases.

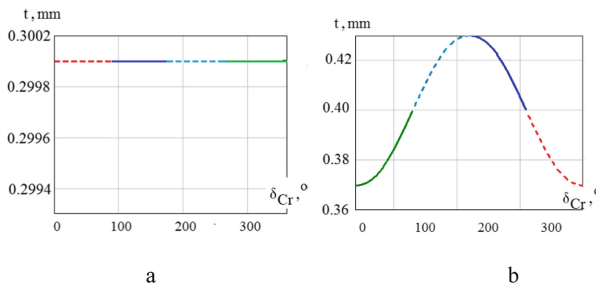


Fig. 8. Graph of distribution of depth of cutting along a contour of a connecting rod neck of a cranked shaft: a – milling with the crossed axes of a mill and details; b – grinding by Junker.

The graph of the distribution of specific productivity Q of machining (Fig. 9) at machining of a cranked shaft with an angle of the crossing of axes of the tool and a detail $\alpha = 1^\circ$, a mill with a diameter of 80 mm and height of a cutting plate of 8,3 mm is received for (9). From the point $xr0$, the graph is developed on the axis coincides with the periphery of a mill's cutting plate.

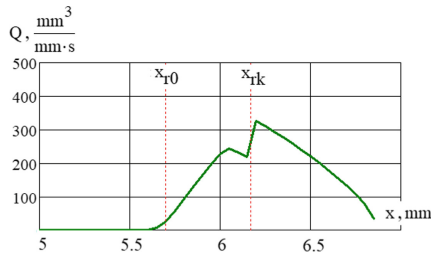


Fig. 9. Distribution of specific productivity Q of milling along with the profile of the cutter tooth.

The largest values of the specific productivity Q of milling (Fig. 9) fall on the area after the coordinate x_{rk} (end of the cutting plate of the cutter), the smallest - the area to the coordinate x_{r0} (periphery of the cutting plate of the cutter) and almost evenly distributed from the coordinate x_{r0} to x_{rk} radial edge of the cutting plate) which is the finishing and calibration area. Removal of the main allowance by an end face of a plate and finishing – by the unloaded periphery of a cutting edge provides an increase of machining accuracy.

For the purpose of uniform wear of quadrilateral plates of a mill at first removal of an allowance from one half of radical and connecting rod necks of a cranked shaft has been carried out, and at the return course of the tool – final machining of necks.

5 Conclusions

Spatial modular models of the tool surface and surface parts have been developed, which give the possibility to analyze the processes of allowance removal and shaping during the milling of a crankshaft root and connecting rod necks.

Based on the developed models, the way of milling of radical and basic necks of crankshafts for one institution where rough milling is carried out by an end face of a quadrilateral plate, and finishing - its unloaded periphery has been offered. The rectilinearity of the shaft necks has been ensured by the displacement of the point of intersection of the tool axes and the part due to the movement of the cutter. The presented method of milling provides stabilization of the depth of cut along with the profile of the connecting rod necks due to synchronous vertical and transverse movement of the cutter with uniform rotation of the crankshaft. The constancy of the depth of cut and reducing the amount of allowance from the end of the plate to its periphery increases the accuracy of shaping the treated surfaces. And milling at the uniform rotation of part gives the chance to increase machining productivity at the expense of increasing the frequency of rotation of a shaft. Milling for the first pass of some halves of necks of a cranked shaft, and for the second – other halves provide uniform wear of plates of the tool.

The proposed method of milling the root and connecting rod necks of the crankshafts can be used to machining various cylindrical surfaces of complex profiles with crossed tool axes and parts on universal sharpening machines with CNC, particular on VZ208F3.

References

1. Zhu, K.: Modeling of the instantaneous milling force per tooth with tool run-out effect in high speed ball-end milling. *Int. J. Mach. Tools Manuf* **118–119**, 37–48 (2017). <https://doi.org/10.1016/j.ijmachtools.2017.04.001>
2. Kar, B.C.: Research trends in high speed milling of metal alloys: a short review. *Mater. Today Proc.* **26(2)**, 2657–2662 (2020). <https://doi.org/10.1016/j.matpr.2020.02.559>
3. Mali, R.A.: A comprehensive review of free-form surface milling – advances over a decade. *J. Manuf. Process.* **62**, 132–167 (2021). <https://doi.org/10.1016/j.jmapro.2020.12.014>
4. Zhu, Z.: High precision and efficiency robotic milling of complex parts: challenges, approaches and trends. *Chinese J. Aeronaut.* 1–25 (2021). <https://doi.org/10.1016/j.cja.2020.12.030>.
5. Pavlenko, I., et al.: Parameter identification of cutting forces in crankshaft grinding using artificial neural networks. *Materials* **13(23)**, 5357 (2020). <https://doi.org/10.3390/ma13235357>
6. Jiang, Z.: Research on stability prediction of the crankshaft CNC tangential point tracing grinding. *Math. Prob. Eng.* **2015**, 1 (2015). <https://doi.org/10.1155/2015/106159>
7. Shen, N., Li, J., Ye, J., Qian, X., Huang, H.: Precise alignment method of the large-scale crankshaft during non-circular grinding. *Int. J. Adv. Manuf. Technol.* **80(5–8)**, 921–930 (2015). <https://doi.org/10.1007/s00170-015-7073-7>
8. Kotliar, A., Gasanov, M., Basova, Y., Panamariova, O., Gubskiy, S.: Ensuring the reliability and performance criterias of crankshafts. *Diagnostyka* **20(1)**, 23–32 (2019). <https://doi.org/10.29354/diag/99605>
9. Yu, H.: In-situ roundness measurement and correction for pin journals in oscillating grinding machines. *Mech. Syst. Sig. Process.* **50–51**, 548–562 (2015). <https://doi.org/10.1016/j.ymsp.2014.05.009>
10. Li, H.L.: Analysis and optimization of milling process for crankshaft pin based on energy consumption. *DEStech Trans. Comput. Sci. Eng.* 355–361 (2019). <https://doi.org/10.12783/dtcse/ica2019/30755>
11. Zhang, M., Yao, Z.: Grinding performance in crankshaft pin journal path-controlled grinding of 40Cr using CBN wheel. *Int. J. Adv. Manuf. Technol.* **82(9–12)**, 1581–1586 (2015). <https://doi.org/10.1007/s00170-015-7473-8>
12. Kalchenko, V.: Development of the single-setup milling process model of the shaft support necks and cams. *Eastern-Eur. J. Enterp. Technol.* **1(106)**, 48–54 (2020). <https://doi.org/10.15587/1729-4061.2020.208579>
13. Rammath, B.V.: Implementation of reverse engineering for crankshaft manufacturing industry. *Mater. Today Proc.* **5(1)**, 994–999 (2018). <https://doi.org/10.1016/j.matpr.2017.11.175>
14. Fan, R.L.: Finite element analysis for engine crankshaft torsional stiffness. *Int. J. Simul. Process Model. (IJSPM)* **14(4)**, 389–396 (2019). <https://doi.org/10.1504/IJSPM.2019.103590>
15. Singh, S.S.K.: Reliability assessment for an automobile crankshaft under random loading. *J. Teknologi (Sciences & Engineering)* **78(6–10)**, 91–96 (2016). <https://doi.org/10.11113/jt.v78.9194>